Earthquakes and Structures, *Vol. 11, No. 5 (2016) 779-807*
DOI: http://dx.doi.org/10.12989/eas.2016.11.5.779

Ground-Motion Prediction Equations based on refined data for dynamic time-history analysis

Salar Arian Moghaddam[a], Mohsen Ghafory-Ashtiany[*] and Mohammadreza Soghrat[b]

International Institute of Earthquake Engineering and Seismology (IIEES), 21 Arghavan st., North Dibajie, Farmanieh, Tehran, Iran

(Received August 17, 2015, Revised September 28, 2016, Accepted September 30, 2016)

Abstract. Ground Motion Prediction Equations (GMPEs) are essential tools in seismic hazard analysis. With the introduction of probabilistic approaches for the estimation of seismic response of structures, also known as, performance based earthquake engineering framework; new tasks are defined for response spectrum such as the reference criterion for effective structure-specific selection of ground motions for nonlinear time history analysis. One of the recent efforts to introduce a high quality databank of ground motions besides the corresponding selection scheme based on the broadband spectral consistency is the development of SIMBAD (Selected Input Motions for displacement-Based Assessment and Design), which is designed to improve the reliability of spectral values at all natural periods by removing noise with modern proposed approaches. In this paper, a new global GMPE is proposed by using selected ground motions from SIMBAD to improve the reliability of computed spectral shape indicators. To determine regression coefficients, 204 pairs of horizontal components from 35 earthquakes with magnitude ranging from Mw 5 to Mw 7.1 and epicentral distances lower than 40 km selected from SIMBAD are used. The proposed equation is compared with similar models both qualitatively and quantitatively. After the verification of model by several goodness-of-fit measures, the epsilon values as the spectral shape indicator are computed and the validity of available prediction equations for correlation of the pairs of epsilon values is examined. General consistency between predictions by new model and others, especially, in short periods is confirmed, while, at longer periods, there are meaningful differences between normalized residuals and correlation coefficients between pairs of them estimated by new model and those are computed by other empirical equations. A simple collapse assessment example indicate possible improvement in the correlation between collapse capacity and spectral shape indicators (ε) up to 20% by selection of a more applicable GMPE for calculation of ε.

Keywords: ground motion prediction; elastic spectral ordinates; correlation; epsilon

1. Introduction

∗Corresponding author, Professor, E-mail: mohsen.ashtiany@gmail.com
[a]Ph.D. Student, E-mail: s.arianmoghaddam@iiees.ac.ir
[b]Ph.D. Student, E-mail: m.soghrat@iiees.ac.ir

 ISSN: 2092-7614 (Print), 2092-7622 (Online)

In common Global Ground Motion Prediction Equations (GMPEs) such as NGA-West2 models, the number of used Ground Motion Records (GMRs) are increased to develop a more acceptable fitted functional form to the data. The basic need to extend the selected database as much as possible can result in the non-uniform reliability of predicted spectral values, especially, in longer periods due to the low quality of recorded accelerograms or reduced number of used data. Several worldwide GMPEs are proposed by using carefully processed accelerograms (Ancheta *et al.* 2014, Cauzzi and Faccioli 2008, Cauzzi *et al.* 2014), however, in most of which the selected database is mainly dominated by recorded data from a specific seismic region which is blended with candidate ground motion records from other sources such that the overall attenuation pattern is preserved. These global models are widely used in earthquake engineering practice, especially, for the estimation of seismic hazard level in a specific site. In probabilistic seismic hazard analysis, the epistemic uncertainty due to the selection of appropriate GMPE is accounted for via multiple weighted GMPEs in logic tree framework. Also, a variety of applicability assessment procedures are proposed to rank the best available GMPE that can predict regional differences (e.g., Scherbaum *et al.* 2009). But, since the order of this type of uncertainty is not comparable to the other sources (e.g., uncertainty in code safety factors) in the result of traditional design process, it has not been quantitatively assessed.

Today with increasing interest in the Nonlinear Time-History Analysis (NLTHA) as a response to the objective of accurate probabilistic assessment of structures in accordance with Performance Based Earthquake Engineering (PBEE) framework, the importance of SGMR selection and modification has been more highlighted. There are a variety of methods proposing efficient selection of SGMRs to be used in the estimation of performance of structure in term of different Engineering Demand Parameters (*EDPs*) (Ghafory-Ashtiany and Arian Moghaddam 2015, Cantagallo *et al.* 2015). Following the PBEE approach, a critical challenge is to simulate nonlinear dynamic collapse under excitation by selected set of SGMs that represent characteristics of extreme ground motions exceeding design levels (Ibarra and Krawinkler 2005) and result in unbiased reliable estimation of *EDPs* at performance levels before collapse. To avoid unreasonable computational effort caused by application of a large number of SGMs in performance assessment process(e.g., collapse simulation), the predetermined sets of SGMs have been refined based on the structure or site specific criteria (e.g., FEMA P.695, Baker *et al.* 2011, Haselton 2006, and Somerville 1997).Considering the fact that near collapse dynamic behavior of structures coincides with high levels of structural softening and consequent period elongation; one can simply conclude that the accuracy and validity of any relationship between ground motion intensity and computed *EDPs* (e.g., maximum inter-story drift ratio) is influenced by the reliability of estimated Intensity Measures (*IMs*) such as elastic spectral ordinates at longer periods. For instance, the meaningful correlation between spectral shape indicators such as Epsilon (Baker and Cornell 2006) and Eta (Mousavi *et al.* 2011) and the collapse capacity of structures is reported (Haselton *et al.* 2009, Mousavi *et al.* 2011). Epsilon measures the deviation of *IM* for a ground motion from the geometric mean of *IM* computed from a GMPE, while Eta is a linear combination of several *IMs*. The concept of spectral shape indicators is generalized toward the development of conditional mean spectrum in Baker (2010), as well as, conditional distribution of other key *IMs* by Bradley (2010). Although, there has been a lot of interest in defining more efficient and sufficient *IMs* among earthquake engineering researchers (e.g., Luco and Cornell 2007, Kwong *et al.* 2015, Konstantinos *et al.* 2015), the elastic spectral ordinates are still the most practically used *IM* due to the some essential unresolved problems in dealing with modern *IMs* such as the intrinsic need to the generation of appropriate GMPE, for example, prediction equations for energy-based *IMs* have

been proposed recently (Cheng *et al.* 2014) or optimum selection of the best GMPE that describes attenuation pattern of the recorded ground motions (Mahmoudi *et al.* 2016). In conclusion, it is mandatory to ensure a fairly uniform improved reliability in the spectral values at whole period range e.g., from 0.1-10s for accurate performance assessment of structures using single or vector-valued *IMs* defined based on the elastic spectral ordinates. In this paper, a new global GMPE is developed for *PGA*, *PGV* and 5%-Damped *PSA* by using selected SGMRs from SIMBAD database which is prepared by Smerzini and Paolucci (2010). The main objective of current study is based on the idea that; if a reliable GMPE can be developed for same set of SGMRs that are used in further researches related to the SGMR selection and modification, introduction of new IMs, and collapse assessment of engineering structures; the interpretation of results are less affected by the epistemic uncertainty initiated from GMPE selection or low accuracy of spectral ordinates. It's worth noting that the main obstacle in this path is the relatively small number of SGMRs compared with available global equations which may yield numerical problems in the convergence of regression procedure.

The construction of SIMBAD has been a precious effort to provide earthquake engineering experts with a database of strong ground motions showing reliable spectral ordinates in a broad range of periods. The original objective of the creation of SIMBAD is to assemble high quality records from different worldwide SGM databases as a basic requirement for displacement based design and assessment of structures in Italy (Smerzini and Paolucci 2010). Third release of database consists of three-component accelerograms refined by checking good signal to noise ratios at long periods. All data were processed by a correction scheme to minimize the possible changes in single and double integration of corrected time series and avoid velocity and displacement time histories with non-zero initial conditions or unphysical baseline trends. Readers are referred to Smerzini and Paolucci (2010) for detailed information about SIMBAD. Although the database has been designed for two structure-specific SGMR selection method based on spectral compatibility (Iervolino *et al.* 2010, Smerzini *et al.* 2014), it has provided researchers with a reliable set of SGMRs, especially, when displacement demand is a key parameter in their study (Graziotti *et al.* 2016). In this study, after the development of an acceptable fitted GMPE to data and verification by several goodness-of-fit measures, the Epsilon value as the spectral shape indicator is computed and the validity of available prediction equations for correlation of the pairs of Epsilon values are examined.

2. Database and methodology

In this study, selected SGMRs from SIMBAD are chosen according to the details presented in Table 1. The dataset comprises of available high quality refined SGMRs from Italy, Greece, Turkey, Iceland, USA, and Newzealand, while, the events with just one recorded station are excluded from the database to allow us compute intra-event errors. In order to determine the regression parameters, the records corresponding to the events presented in Table 1 are employed for the analysis. The dataset, which includes 204 pair of horizontal components, is used for computing Pseudo-spectral Acceleration (*PSA*), Peak Ground Acceleration (*PGA*) and Peak Ground velocity (*PGV*) from the recordings of the 35 earthquakes, whose range of moment magnitude (M_W) is 5-7.1. There are 33, 82 and 89 records on A, B, and C site classes, respectively, while 7 records on soil type of D are eliminated to reduce the dispersion in regression results. It should be noted that site classification is based on Eurocode 8 (CEN 2004) by using V_{S30}

measurements (48%) or definition of the site class based on quantitative criteria (52%). Also, 48, 46, 54, and 56 records correspond to the reverse, normal, strike-slip and unknown fault mechanisms, respectively. The distributions of magnitude-distance of the selected events are plotted in Fig. 1. As it can be seen in the figure, the database is rich at available magnitudes and distances, where no obvious gap exists in data. Among different distance definitions, we have used the epicentral distance, as the distance parameter for all the earthquakes studied in this research.

Table 1 Earthquakes analyzed in the present study

No.	Event_Name	Event_Date	Event_Time	Area	Mw	N*	Fault type
1	Friuli 2nd shock	1976_September_11	16:35	Italy	5.6	3	reverse
2	Friuli 3rd shock	1976_September_15	03:15	Italy	5.9	2	reverse
3	Friuli 4th shock	1976_September_15	09:21	Italy	5.9	3	reverse
4	Imperial Valley	1979_October_15	23:16	USA	6.5	6	strike-slip
5	Irpinia	1980_November_23	18:34	Italy	6.9	3	normal
6	Loma Prieta	1989_October_18	00:04	USA	6.9	7	oblique
7	Northridge	1994_January_17	12:30	USA	6.7	7	reverse
8	Kozani_aftershock	1995_May_15	04:13	Greece	5.2	2	odd
9	App.Umbro-Marchigiano	1998_March_21	16:45	Italy	5	2	normal
10	Duzce	1999_November_12	16:57	Turkey	7.1	3	strike-slip
11	Duzce	1999_November_12	16:57	Turkey	7.1	4	strike-slip
12	Athens_mainshock	1999_September_07	11:56	Greece	6	3	odd
13	South Iceland	2000_June_17	15:40	Iceland	6.5	4	strike-slip
14	South Iceland	2000_June_21	00:51	Iceland	6.4	9	strike-slip
15	Parkfield	2004_September_28	17:15	USA	6	4	strike-slip
16	Parkfield	2004_September_28	17:15	USA	6	8	strike-slip
17	Anza	2005 June 12	15:41	USA	5.2	5	strike-slip
18	Olfus	2008_May_29	15:45	Iceland	6.3	3	strike-slip
19	L'Aquila mainshock	2009_April_06	01:32	Italy	6.3	5	normal
20	L'Aquila aftershock	2009_April_06	02:37	Italy	5.1	2	normal
21	Gran Sasso	2009_April_06	23:15	Italy	5.1	2	normal
22	L'Aquila aftershock	2009_April_07	09:26	Italy	5	4	normal
23	L'Aquila aftershock	2009_April_07	17:47	Italy	5.6	8	normal
24	L'Aquila aftershock	2009_April_09	00:52	Italy	5.4	8	normal
25	L'Aquila aftershock	2009_April_09	19:38	Italy	5.3	7	normal
26	L'Aquila aftershock	2009_April_13	21:14	Italy	5.1	5	normal
27	Darfield	2010_September_03	16:35	NewZealand	7.1	8	strike-slip
28	Christchurch	2011_February_21	23:51	NewZealand	6.2	9	reverse
29	Christchurch	2011_February_22	00:04	NewZealand	5.5	8	odd
30	Christchurch	2011_February_22	01:50	NewZealand	5.6	7	odd
31	Christchurch	2011_June_05	21:09	NewZealand	5.1	12	odd

Table 1 Continued

No.	Event_Name	Event_Date	Event_Time	Area	Mw	N*	Fault type
33	Christchurch	2011_June_13	02:20	NewZealand	6	10	reverse
34	Christchurch	2011_June_21	10:34	NewZealand	5.2	10	odd
35	EMILIA_Pianura_Padana	2012_May_29	07:00	Italy	6	14	reverse

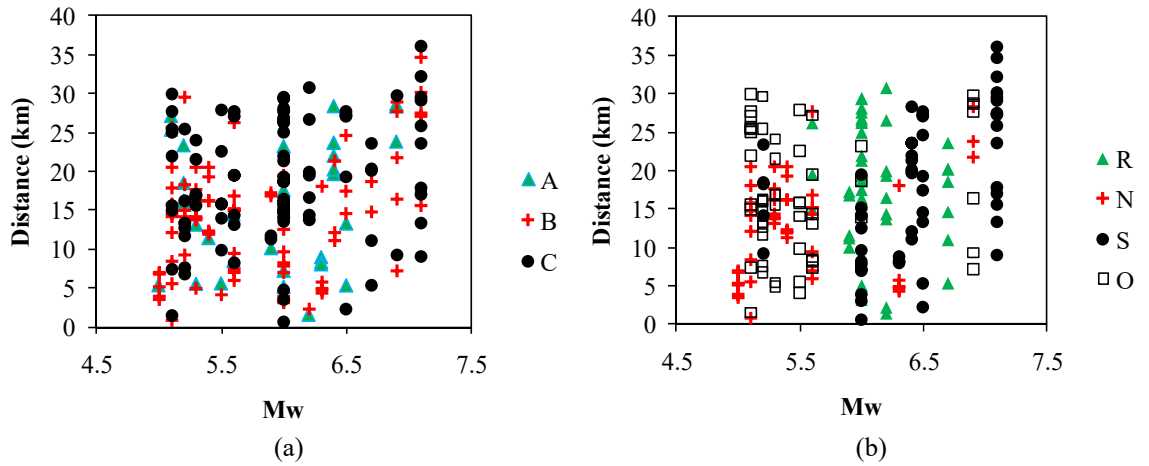

Fig. 1 M Distribution of moment magnitude, distance versus site classification (a) and fault type (b). S=strike-slip; N=normal; R=reverse; O=oblique and odd represent unknown fault type

To select the best functional form for GMPEs, several proposed and successfully applied general equation forms in the literature have been examined as shown in Table 2 in association with references in which they are applied (Akkar and Bommer 2007, 2010, Ghodrati Amiri *et al.* 2009, Ghasemi *et al.* 2009), where *IM* denotes the selected intensity measure (*PGA*, *PGV*, etc.), b1-b12 are coefficients that must be determined using regression analysis (these coefficient are period dependent in case of spectral *IMs*). M_W and R represent moment magnitude and epicentral distance, respectively. From the given equations in Table 1, the first one which is generalized form of the equation by Akkar and Bommer (2007, 2010), is selected because it produces the least regression errors among all of the five equations. To account for different site classes, variables *SA* and *SS* are used as follows; *SA* and *SS* are equal to 1 for stiff ($360<V_{s30}<800$) and soft soil ($180<V_{s30}<360$) sites, respectively, and zero otherwise. Effect of the faulting style is modeled using variables F_N, F_R, F_S, and F_{Odd} which are representing the normal, reverse, strike-slip and unknown mechanisms, respectively. In each case of faulting, the corresponding variable takes the value of 1 while the others are equal to zero.

3. Regression analysis and results

Regression of the dataset is carried out in accordance with the maximum likelihood method. Following this approach, two most important issues should be considered: the problem of weighting observations from different events, and to prevent the events with a large number of

recordings from producing the biased model parameters. The fixed-effects model is the traditional approach for deriving attenuation relationships as the empirical equations fitted to the earthquake data. Trying to reduce the bias associated with the random distribution of records; Brillinger and Preisler (1984, 1985) have proposed a random-effects model to distinguish the uncertainties caused by inter-event (earthquake-to-earthquake) and intra-event (record-to-record) variations. Therefore, the error terms in model are divided into intra-event and inter-event types. The more stable algorithm of Abrahamson and Youngs (1992) for maximizing the likelihood function in the random effect model is used here, while there are many successful applications of it in the literature (Soghrat *et al.* 2012, Zafarani and Soghrat 2012).

The regression model is given as

$$\log y_{ij} = \log \mu_{ij} + \eta_i + \varepsilon_{ij} \tag{1}$$

In which y_{ij} represents the geometric mean of intensity measures (*PSA, PGA* and *PGV*) as obtained from data, and μ_{ij} shows the predicted measures for data point *j* of event *i*. It is assumed that the intra-event (ε_{ij}) and inter-event (η_{ij}) error terms are independent zero-mean normally-distributed, random variables with variance of σ_e and σ_r, respectively. For a given set of regression parameters, the residuals are determined as the following form

$$res(\theta)_{ij} = \log \frac{y_{ij}}{\mu(\theta)_{ij}} \tag{2}$$

The residuals are defined as the differences between the logarithms of the observed and predicted *IMs* including spectral values for 21 periods distributed based on the format of NGA-GMPEs between 0.01 and 10s, in addition to the PGA and PGV. The total standard deviation (σ_T) is given by Eq. (3) knowing that inter-event (σ_e) and intra-event (σ_r) components both participate in generation of σ_T

$$\sigma_T = \sqrt{\sigma_e^2 + \sigma_r^2} \tag{3}$$

In each iteration of the random effects procedure the best estimate of the model parameters θ

Table 2 Different equation forms examined in present study

No.	Equation form	References
1	$Log_{10}(IM) = b_1 + b_2 M_W + b_3 M_W^2 + (b_4 + b_5 M_W) Log_{10}\sqrt{R^2 + b_6^2} + b_7 S_S + b_8 S_A + b_9 F_R + b_{10} F_N + b_{11} F_S + b_{12} F_{Odd}$	Present study
2	$Log_{10}(IM) = b_1 + b_2 M_W + b_3 M_W^2 + (b_4 + b_5 M_W) Log_{10}\sqrt{R^2 + b_6^2} + b_7 S_S + b_8 S_A$	Akkar and Bommer (2007, 2010)
3	$Log_{10}(IM) = b_1 + b_2 M_W + b_3 M_W^2 + (b_4 + b_5 M_W) Log_{10}\sqrt{R^2 + b_6^2}$	Simplified form of Akkar and Bommer (2007, 2010)
4	$Log_{10}(IM) = b_1 + b_2 M_W + b_3 Log_{10}(R)$	Ghodrati *et al.* (2009)
5	$Log_{10}(IM) = b_1 + b_2 M_W + b_3 Log_{10}(R + b_4 \times 10^{b_5 \times M_w}) + b_6 S_S + b_7 S_A$	Ghasemi *et al.* (2009)

must be estimated, which may be found by minimizing the following form

$$\Gamma = \left(\sum_{i=1}^{N_e} \sum_{j=1}^{N_r . N_T} [res_{ij}(\theta)]^2 \right)^{0.5} \tag{4}$$

Where, N_e, N_r, and N_T are the number of earthquake events, observations and discrete oscillator periods in case of spectral *IMs*, respectively. Random effects are assumed for all 12 coefficients, i.e., no one is treated as purely fixed effect. Following the latter assumption; no computational difficulty occurred to be alleviated by using a necessarily fixed parameter. Coefficient "b_6" is referred to as a "fictitious" depth measure and its values can be computed as a part of the regression (Abrahamson and Youngs 1992).

Table 3 presents results of the nonlinear regression analysis for the estimation of coefficients as well as variance components in case of *PGA* (cm/s^2), *PGV* (cm/s^2) and *PSA* (cm/s^2) at periods ranging from 0.01 to 10 s. Aleatory variability in the predicted *IMs* is in acceptable range based on the estimated total variance plotted in Fig. 2. To assess the possible influence of the limited size of

Table 3 Coefficients and Statistical Parameters computed from the Regression Analysis

T	b_1	b_2	b_3	b_4	b_5	b_6	b_7	b_8	b_9	b_{10}	b_{11}	b_{12}	σ_e	σ_r
PGA	1.7707	1.0701	-0.1278	-5.5555	0.6524	12.0470	0.0539	0.2551	0.6996	0.3348	0.6715	0.7474	0.0949	0.2258
0.01	1.7131	1.0706	-0.1242	-5.3198	0.6181	11.7474	0.0487	0.2518	0.5878	0.2203	0.5646	0.6318	0.0949	0.2261
0.02	1.8358	0.9986	-0.1152	-5.0711	0.5843	11.4961	0.0292	0.2365	0.5289	0.1620	0.5120	0.5665	0.1025	0.2269
0.03	1.7844	0.8746	-0.0988	-4.6492	0.5228	10.6970	-0.0017	0.2230	0.6838	0.3199	0.6742	0.7097	0.1095	0.2258
0.05	2.8015	0.6737	-0.0813	-4.6468	0.5176	10.1422	-0.0567	0.2028	0.3617	0.0620	0.3480	0.4104	0.1086	0.2400
0.075	1.7831	0.8275	-0.0839	-3.9285	0.4178	8.9278	-0.0674	0.2114	0.4786	0.1724	0.4735	0.5388	0.0849	0.2421
0.1	1.2510	1.2486	-0.1322	-4.8682	0.5466	11.2394	-0.0396	0.2259	0.5547	0.2415	0.5500	0.6337	0.0872	0.2480
0.15	1.9162	1.1850	-0.1361	-5.6622	0.6639	12.1882	0.0759	0.3197	0.5281	0.1760	0.4468	0.6132	0.0583	0.2526
0.2	0.9145	1.2989	-0.1384	-5.2137	0.6326	10.7281	0.1545	0.3552	0.5020	0.1524	0.4261	0.5695	0.0714	0.2602
0.25	0.5213	1.7065	-0.1853	-6.3344	0.7765	12.7338	0.2550	0.3722	0.4216	0.1553	0.3843	0.5202	0.0608	0.2665
0.3	-1.5079	2.1786	-0.2146	-5.7659	0.7149	11.0863	0.3085	0.3831	0.3343	0.0827	0.2813	0.4650	0.0500	0.2830
0.4	-3.1156	2.9031	-0.2873	-6.9298	0.8662	12.7369	0.3781	0.3879	0.4757	0.2889	0.4444	0.6404	0.0510	0.2902
0.5	-5.5080	3.3644	-0.3051	-5.8906	0.7008	11.1910	0.3987	0.3622	0.5816	0.3789	0.5443	0.7085	0.0800	0.2905
0.75	-5.5081	3.7507	-0.3526	-7.3592	0.8572	14.1774	0.4625	0.2988	0.5825	0.4442	0.5593	0.6272	0.1375	0.2665
1	-3.4251	3.9019	-0.4055	-9.9789	1.2189	19.2173	0.4569	0.2566	0.1176	0.0796	0.1263	0.1874	0.1334	0.2587
1.5	-8.0849	4.4767	-0.4075	-7.7825	0.9249	17.1303	0.4706	0.2414	0.4951	0.4493	0.4822	0.5705	0.1127	0.2678
2	-9.6646	5.2597	-0.4909	-8.6758	1.0870	17.2528	0.4575	0.1870	0.1262	0.1124	0.1456	0.1725	0.1131	0.2696
3	-13.8412	5.6988	-0.4897	-6.4287	0.8225	13.1752	0.4559	0.1615	0.3550	0.2663	0.4051	0.3539	0.1315	0.2713
4	-9.3377	4.8408	-0.4637	-9.0529	1.2206	16.4952	0.4647	0.1581	0.2229	0.1174	0.3006	0.2428	0.1449	0.2653
5	-8.5965	4.3632	-0.4202	-8.7957	1.1973	16.8415	0.4826	0.1775	0.3888	0.2917	0.5035	0.4408	0.1584	0.2746
7.5	-6.3534	3.0929	-0.2935	-7.6771	1.0603	14.7771	0.4904	0.2049	0.3074	0.1692	0.4737	0.3507	0.1418	0.2753
10	-7.6854	3.2406	-0.2970	-7.3109	0.9912	13.1948	0.4626	0.2049	0.6055	0.4742	0.7594	0.6489	0.1292	0.2666
PGV	-4.2389	2.8050	-0.2725	-6.7786	0.8335	13.0030	0.2808	0.2432	0.4661	0.2478	0.4947	0.5297	0.1145	0.2362

dataset in present study, Fig. 2 depicts the difference among different components of standard deviation in our model compared with the proposed GMPE by (Bindi *et al.* 2014a, b), which is abbreviated as Bea14 hereafter. It is clear from this figure that the proposed model produces acceptable standard deviation compared to a similar recently published equation which is developed for RESORCE dataset (including 1224 records). It should be noted that the mean value of standard deviations for spectral values over the whole periods in our model is 0.288, which shows a reduction about 25% when it compares with 0.357 from (Bindi *et al.* 2014a, b).

As it is can be seen in Fig. 2, the mentioned reduction is mainly originated from the difference between inter-event errors in two models. When one may expect the more statistical dispersion in SIMBAD database due to the variety of sources from which the ground motions are selected; the observed lower dispersion, implicitly, confirms effective homogeneity in our data collected from different sources all around the world. The predicted acceleration spectra for several magnitudes and source distances at different site classes are shown in Fig. 3. One can simply observe the variation of spectral shape with site classes in the figure that shows the increase in spectral amplitudes at longer periods for the softer site conditions. In other words, no specific trend can be concluded describing the uniform effect of the soil types on the amplification of spectral values at all period ranges. This is in agreement with the results of comprehensive investigations done for NGA-West2 database (Campbell and Bozorgnia 2008) which confirms different possible patterns for soil amplification due to the nonlinear site effects.

Fig. 4 presents acceleration spectra derived from our model for several magnitudes and source distances using different faulting styles. It can be concluded that the spectral values at lower periods are more sensitive to the style of faulting. While the normal faulting shows the most deviation, this sensitivity decreases gradually by approaching longer periods. Fig. 5 illustrates the comparison between observed data and median predictions of the proposed model for different magnitudes and site classes. The moment magnitude of 5.2 rather than 5 is considered in this figure, to increase the number of observed points in the determined tolerance of M_W and for fixed faulting style.

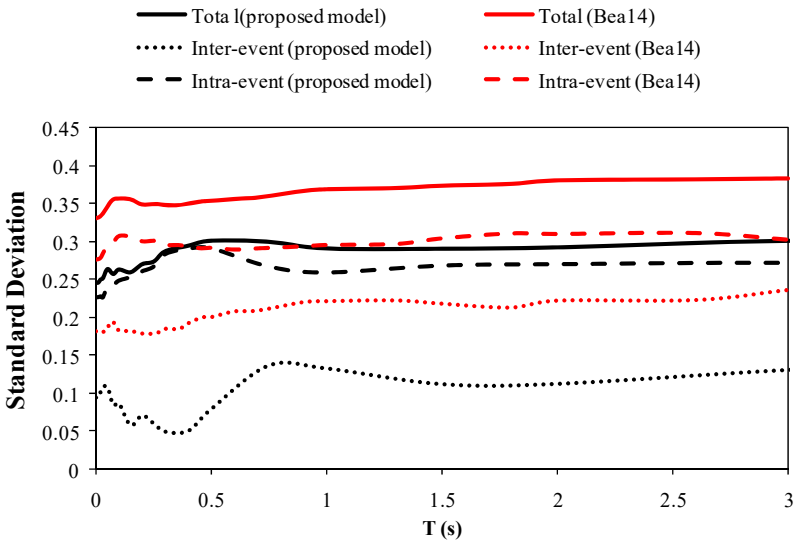

Fig. 2 Comparison of the standard deviation components between the proposed model and Bea14

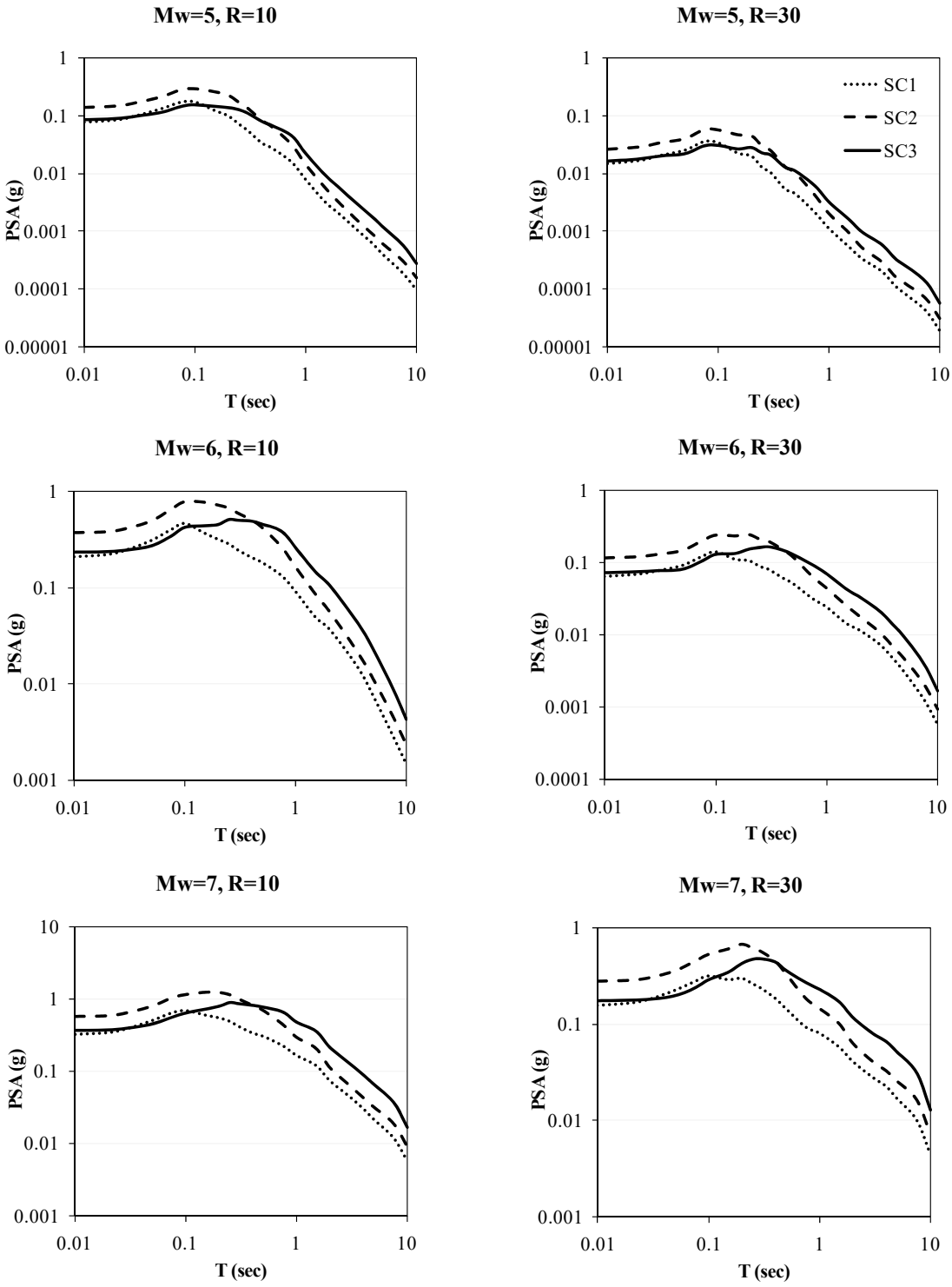

Fig. 3 Predicted PSA for Mw=5, 6, 7 and epicentral distance of 10 and 30 km for site classes (SC 1, SC 2, SC3). The fault mechanism is assumed to be strike-slip (most recorded type; 55 records)

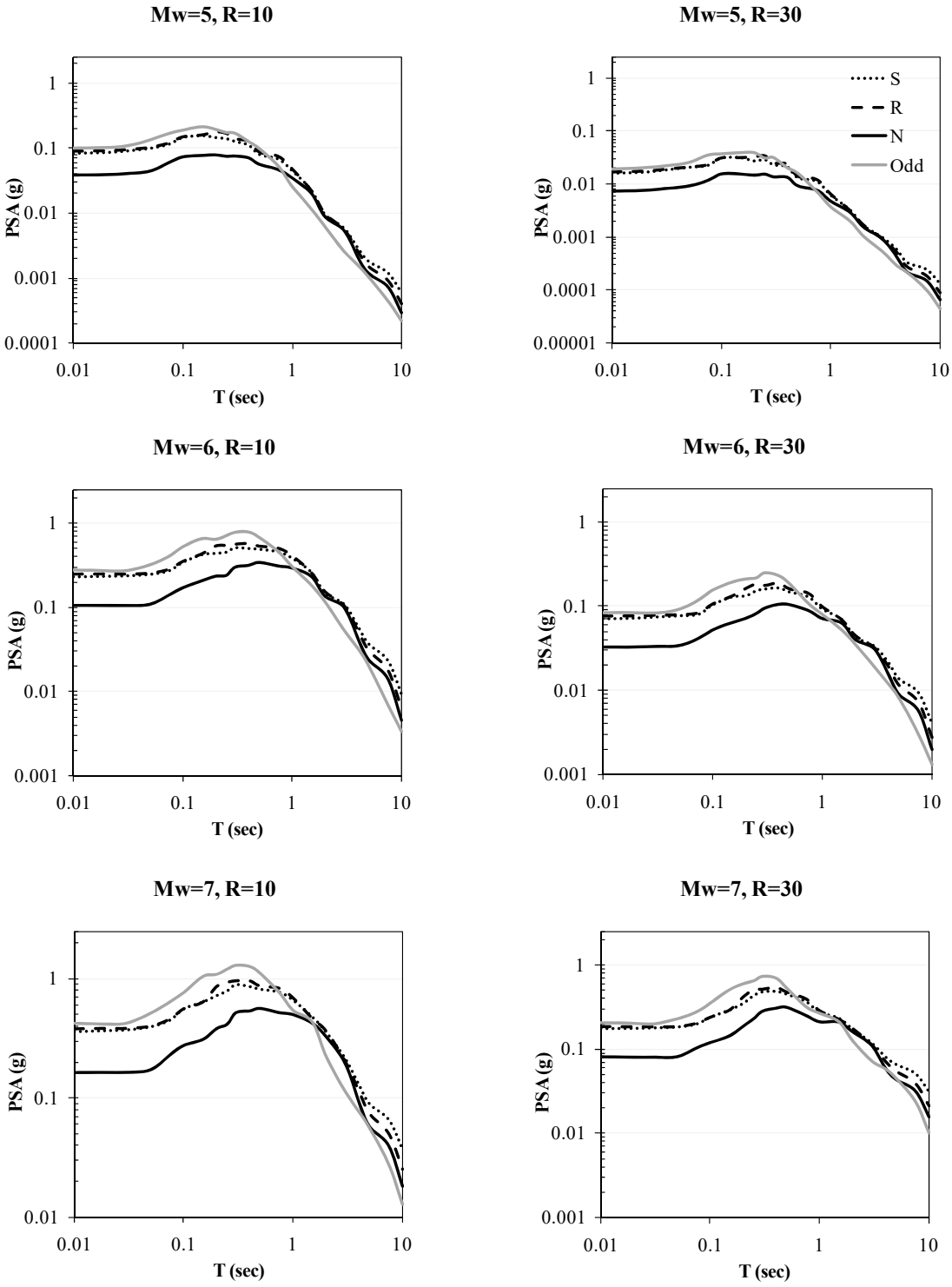

Fig. 4 Predicted PSA for Mw=5, 6, 7 and epicentral distance of 10 and 30 km for four fault mechanisms (S, R, N and Odd). The site class is assumed to be or SC3 (most recorded type; 89 records)

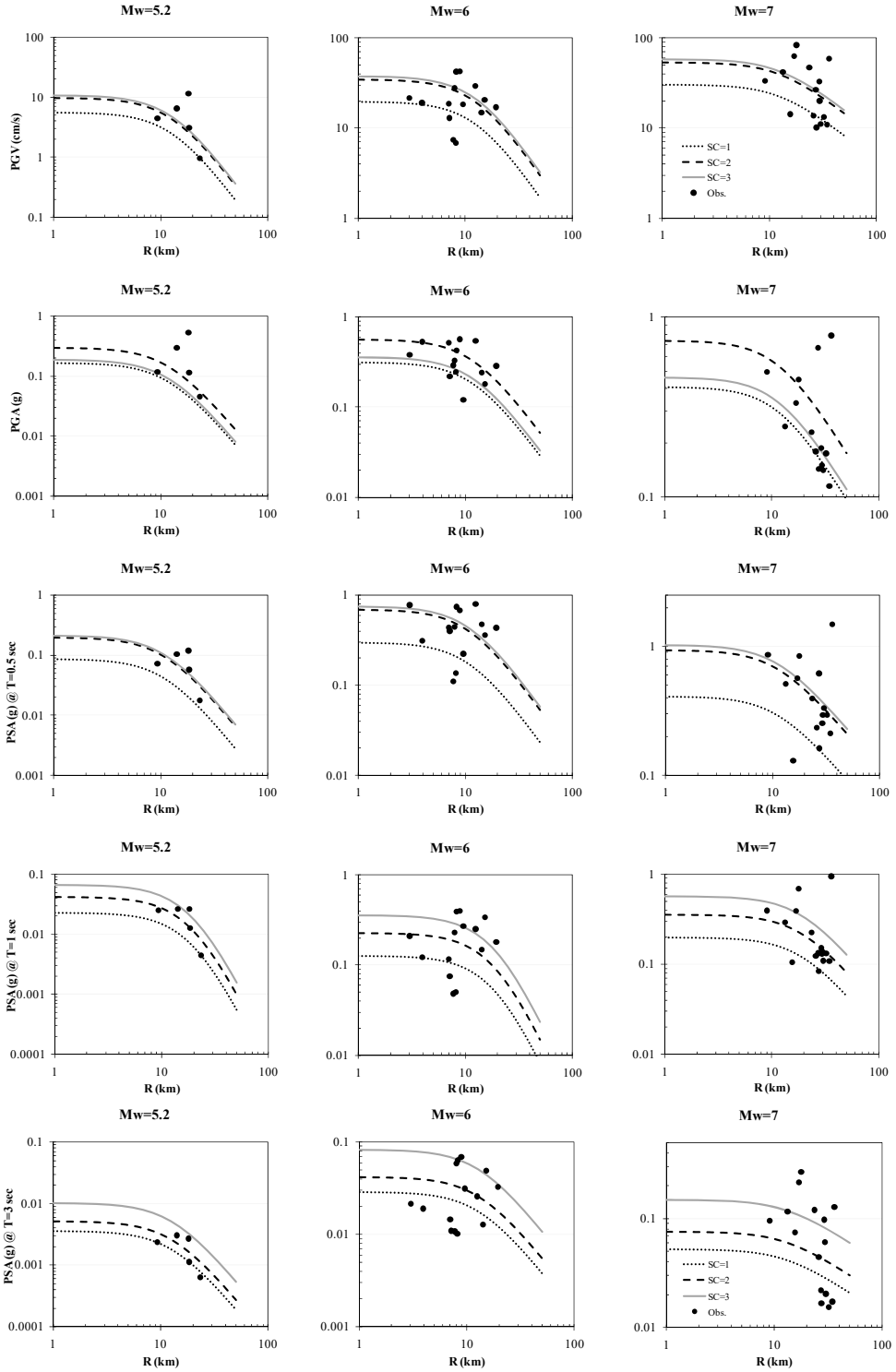

Fig. 5 Comparison of proposed equations for different site classes with the observed data (considering a tolerance of ±0.3 in Mw)

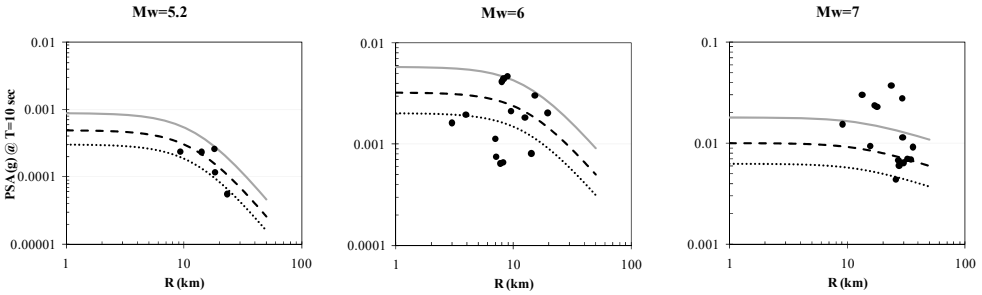

Fig. 5 (Continued)

4. Residual analysis

The accuracy of the proposed GMPE is validated by means of residual analysis in this section. The inter-event and intra-event residuals are shown in Figs. 6-7. These figures enable us to show a qualitative appreciation for the distribution of the residuals. It can be seen that the error terms do not show any systematic trend with respect to the magnitude and distance parameters, and the slope of the fitted trend-line is approximately zero. The fact that the residuals show zero-mean distribution un-correlated to the independent regression parameters confirms the ability of proposed model in un-biased prediction of *IMs* (Campbell and Bozorgnia 2003). To evaluate the quality of fitted model to the selected data, histograms of the residuals are plotted in Fig. 8 for *PGV*, *PGA* and *PSA* at periods of 0.5, 1 and 3s. The normal Probability Distribution Function (PDF) which is expected for each set, on the basis of the obtained standard deviations of each model, is illustrated by thick solid lines. Moreover, the PDF fitted to each set of residuals is represented by dashed line. To validate the results, the model of Bea14, is compared with the proposed model. As it is obvious from Fig. 8, the expected and estimated PDFs match well for the proposed model, while the model of Bea14 can represent our data approximately. To quantitatively evaluate the effectiveness of the model in predicting *IMs*, different statistical goodness-of-fit measures are utilized. The first method is the Nash–Sutcliffe efficiency coefficient (Nash and Sutcliffe 1970), which is given as follows

$$EC = \left[1 - \frac{\sum_{i=1}^{N} (LnY_i - Ln\widehat{Y}_i)^2}{\sum_{i=1}^{N} (LnY_i - \overline{LnY_i})^2} \right] \tag{5}$$

Where N is the total number of predictions, observations (*PGA, PGV*, etc.) are denoted by Yi, the median values of predictions are denoted by $\overline{Yi}$ and the mean of the logarithms of the observations is denoted by $(\overline{LnYi})$. The higher values of *EC* (close to 1) reveal better agreement between observations and predictions, e.g., a perfect match between predicted and observed values (all residuals equal to zero) results in *EC*=1. The results are presented in Table 4 for *PGA*, *PGV*, and spectral acceleration at representative periods of 0.5, 1, and 3s (to be comparable with the model of Bea14). Although, the mentioned evaluations confirm the prediction ability of proposed model, *LH* method (Scherbaum *et al.* 2009) is used to involve standard deviation relationships in the accuracy assessment procedure. The *LH* value for a GMPE, by assumption of zero mean and

unit variance, is given as

$$LH(|Z_0|) = Erf\left(\frac{|Z_0|}{\sqrt{2}}, \infty\right) = 1 - Erf\left(\frac{|Z_0|}{\sqrt{2}}\right) \tag{6}$$

$$Erf(|Z_0|) = \frac{2}{\sqrt{\pi}} \int_0^{Z_0} e^{-t^2} dt, \tag{7}$$

In which *Erf* is the error function and Z_0 is the normalized model residual. Since the ground-motion models are commonly expressed as the natural logarithmic quantities, the residual is defined as the subtraction of the natural logarithmic-model predictions from the natural logarithms of the observed values, divided by the corresponding standard deviations of the natural logarithmic model. This parameter is known also as a spectral shape indicator Epsilon (ε) that is studied more in the coming sections.

Ideally, the defined residual is normally distributed with zero mean and unit variance. If these assumptions are true for a subset of predictions, the *LH* values are uniformly distributed between 0 and 1. If the mentioned distribution matches a perfect standard normal distribution with the zero mean and the unit variance, then the corresponding *LH* has a median value close to 0.5. The mean, median and standard deviation of the normalized residuals, as well as median *LH* are reported in Table 4, and Fig. 9 shows the *LH* distributions for two models in representative periods. Results of all goodness-of-fit measures summarized in Table 4 prove the superiority of proposed model in predicting *IMs*, while the model of Bea14 is, also, an acceptable GMPE for selected dataset in this paper.

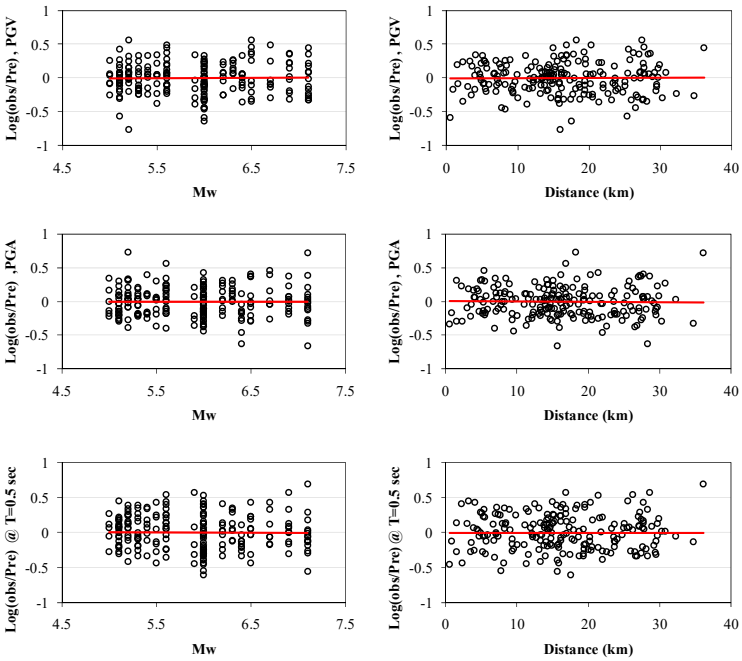

Fig. 6 Intra-event residuals as a function of distance and magnitude

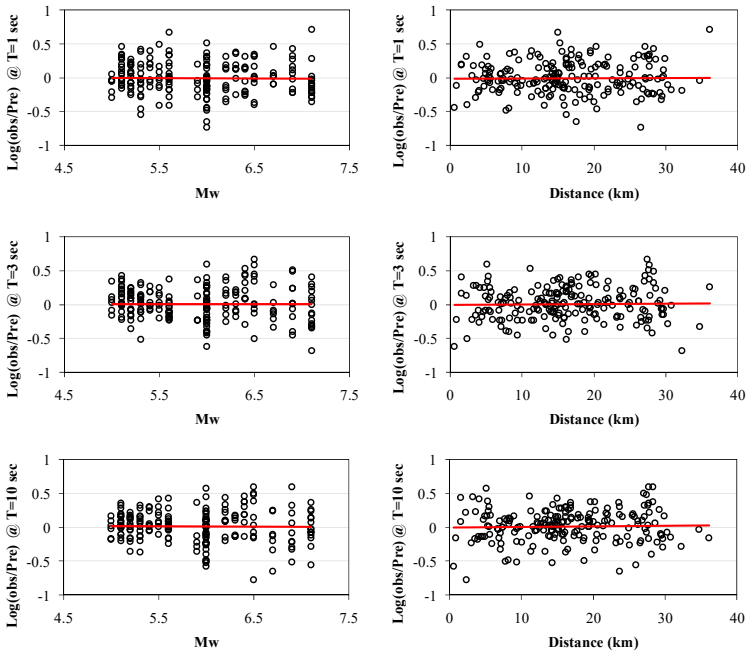

Fig. 6 Continued

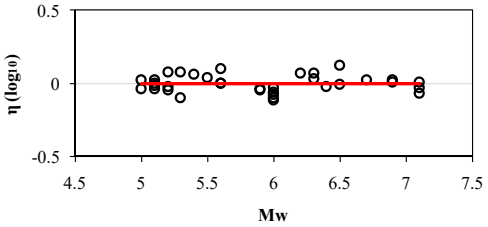

Fig. 7 Inter-event residuals as a function magnitude

Table 4 The results of goodness-of-fit measures on the used database

T	EC		MEDLH		MEANNR		MEDNR		STDNR	
	Bea14	New model	Bea14	New model	Bea14	New model	Bea14	New model	Bea14	New model
PGV	0.593	0.731	0.574	0.521	-0.085	-0.012	-0.114	-0.022	0.827	0.988
0	0.548	0.721	0.578	0.490	0.361	-0.016	0.322	-0.024	0.870	0.997
0.5	0.530	0.681	0.476	0.494	0.419	-0.013	0.412	0.077	0.944	0.999
1	0.685	0.751	0.636	0.506	0.205	-0.028	0.203	-0.074	0.859	0.992
3	0.728	0.787	0.545	0.530	0.081	0.013	0.197	0.067	0.882	0.994
				No. of records				**No. of event**		
	New model			204				35		
	Bea14			1224				255		

Note: The selected measures of goodness-of-fit are: Efficiency Coefficient (EC), Median LH values (MEDLH) and (MEANNR), (MEDNR) and (STDNR) denote Mean, Median and Standard Deviation of the Normalized Residuals, respectively.

Unfortunately, Bea14 is not developed for periods longer than 3s which this paper has focused on to improve the reliability of spectral ordinates. Although, the applicability assessment of candidate GMPEs for any new datasets needs a separate comprehensive framework (Kaklamanos and Baise 2011) that is not in the scope of present study, the Bea14 has been selected as an acceptable GMPE for selected data based on the results of our preliminary evaluations. Several other global GMPE failed to represent the data in term of the normality of residuals, probably, due to the presence of strong regional dependencies or the inconsistency caused by large number of data recorded at far distances (R>50 km). It is worth noting that the data used in present study includes 83% less records than Bea14 from more variable sources.

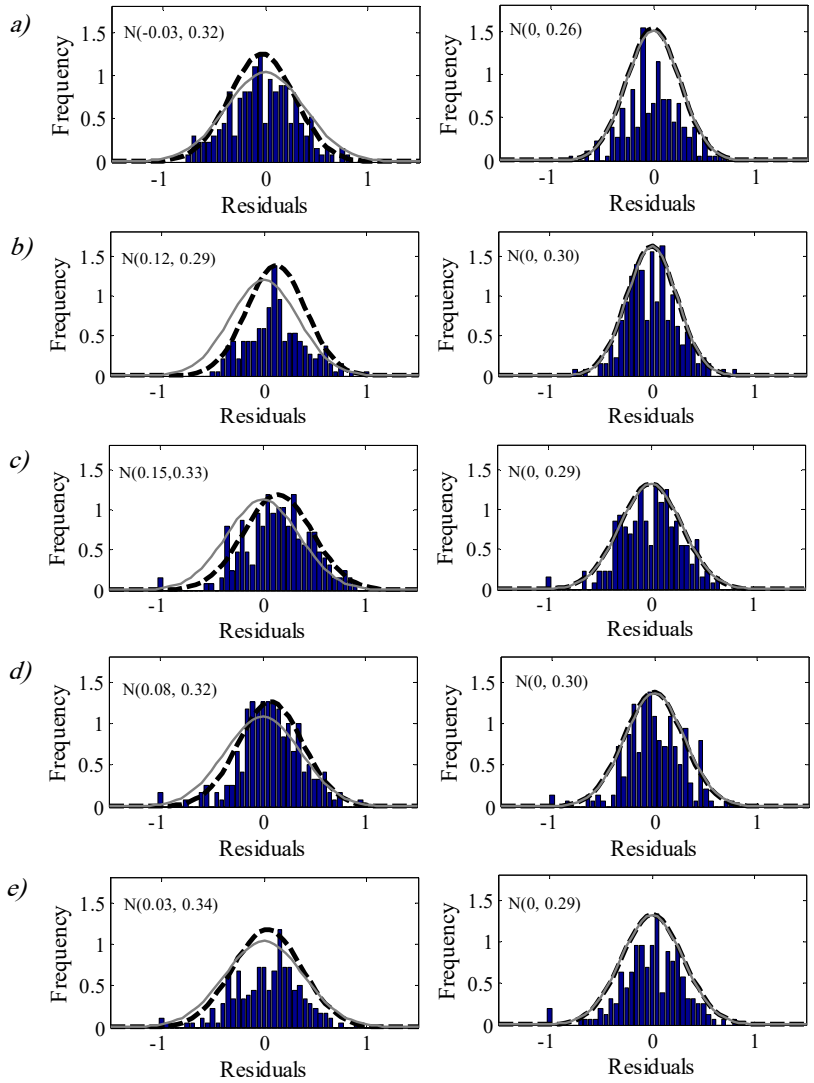

Fig. 8 Residual histograms for the proposed model (right) and the model of Bea14 (left) at PGV (a), PGA (b) and PSA at periods of 0.5 sec (c), 1 sec (d) and 3 sec (e). The values in parentheses in each graph are, respectively, the mean and standard deviation of the fitted normal distribution

4. Comparison of proposed model with others

A comparison for median predicted values (*PGV*, *PGA* and *PSA*) based on the proposed ground-motion model with those computed by other available GMPEs in the literature is done to show the validity of the model.

Table 5 Characteristics of GMPEs compared with proposed model

Study	Abbreviation	Region	$(N_R, N_E)^*$	M^{**}	M_{Min}, M_{Max}	R^{***}	R_{min}, R_{max}
Ambraseys and Douglas (2003)	AD03	Worldwide	(186, 42)	Ms	5.8, 7.8	R_{jb}	0, 15
Rupakhety *et al.* (2011)	Rea11	Worldwide	(93, 29)	Mw	5.5, 7.6	R_{jb}, R_{epi}	0, 30
Bindi *et al.* (2014)	Bea14	Europe and the Middle East	(1224, 365)	Mw	4, 7.6	R_{jb}, R_{hypo}	0, 300
Campbell and Bozorgnia (2014)	CB14	Worldwide	(15521, 322)	Mw	3.3, 8.5	R_{rup}	0, 300
Boore *et al.* (2014)	BOea14	Worldwide	(~16000, ~300)	Mw	3, 7.9	R_{jb}	0, 400

$^*N_R$ and N_E refer to number of records and number of events, respectively.
**Ms and Mw denote surface magnitude and moment magnitude, respectively.
*** R_{jb}, R_{epi}, R_{hypo} and R_{rup} indicate closest distance to horizontal projection of rupture surface, epicentral distance, hypocentral distance and closest distance to rupture surface.

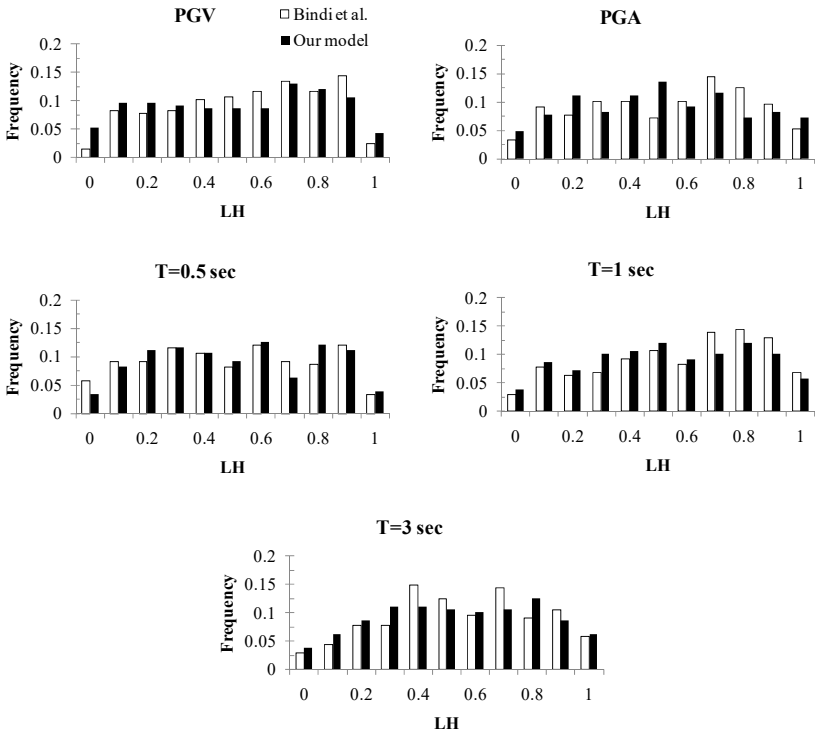

Fig. 9 Comparison of LH distributions for two models

Table 5 shows characteristics of GMPEs that are used for the comparison. These global GMPEs are selected to cover a variety of applicability limits for magnitude, distance as well as size of used dataset for development of them; (Bindi *et al.* 2014a, b), Campbell and Bozorgnia (2014), and Boore *et al.* (2014) represent general worldwide equations developed by using large data whose epicentral distances are extended up to 365 km. In addition, Since the SIMBAD comprises of SGMRs recorded at distances up to 40 km, the model of Ambraseys and Douglas (2003) for near-field ground motions is used, too. Furthermore, a mathematical relationship that is proposed by Rupakhety *et al.* (2011) to quantify the characteristics of near-field pulse-like SGMRs is added; however, there has not been any specific evaluation on the current database focusing on directivity velocity pulses.

Fig. 10 illustrates comparison among selected GMPEs for epicentral distances ranging from 1 km to 50 km and for a constant moment magnitude (M_w=6) at soil class C and faulting mechanism of strike-slip. The overall shape of model presented in this study is similar to the other GMPEs, with spectral ordinates higher than others with the exception of CB14 (at short distances). The predictions of Rea11 relationship severely deviates from others in distances more than 15 km and longer periods. Although there is a fairly good agreement in *PGV* predictions, none of the models can be used as an alternative for Rea11 in case of pulse-like ground motions. Sensitivity of spectral ordinates to the selected GMPE is increased for longer periods. There is a good agreement between our model and BOea14 at T=10s; as well as *PGV* and *PGA* that is not observed for T=3, 4, 5, and 7.5s (just T=3s is plotted in Fig. 10 for brevity).

5. Blind test on a set of SGMRs refined for NLTHA

As it was explained in the introduction, increasing interest in PBEE has led to the special attention paid to the selection and modification of SGMRs as the input of NLTHA. To avoid expensive computational cost caused by large number of randomly selected SGMRs, different predefined sets of records have been developed in seismic guidelines, provisions, and benchmark research reports. These datasets that are refined based on the structure specific criteria may differ from large ordinary datasets by which the GMPEs are developed. In this section a blind test is conducted to evaluate the performance of our model and Bea14 using set of 39 SGMRs proposed in Haselton (2006), which has been widely used in NLTHA or performance assessment of structures.

It should be noted that only data from distance and magnitude range consistent with present study are used. The goodness-of-fit measures introduced in section 3 are utilized again to quantify

Table 6 results of goodness-of-fit measures for blind test

T	MEDLH		MEANNR		MEDNR		STDNR	
	Bea14	Our model	Bea14	Our model	Bea14	Our model	Bea14	Our model
PGV	0.452	0.675	-0.750	0.053	-0.753	0.018	0.419	0.565
0	0.588	0.623	0.544	0.345	0.543	0.437	0.441	0.628
0.5	0.499	0.662	0.731	0.391	0.677	0.333	0.502	0.486
1	0.705	0.656	0.405	0.143	0.352	-0.068	0.602	0.771
3	0.744	0.606	-0.104	-0.215	-0.230	-0.063	0.690	0.790

the level of the applicability of models. Based on the results summarized in Table 6, the normality of our model is better than Bea14 in terms of mean, median and standard deviation of the normalized residuals. Based on the *LH* results, Bea14 is slightly better predictor of spectral values at lower periods, while this superiority diminishes rapidly at longer periods. Fig. 11 compares the prediction performance of our model and Bea14 for main used database and the blind test set.

6. Practical example

The ability of spectral shape indicators such as Epsilon and Eta in predicting the potential of a SGMR to cause structural collapse has been analyzed and it was shown that that there is a meaningful correlation between natural logarithm of $Sa(T_1)_{COL}$ vs. $\varepsilon(T_1)$, which can be used

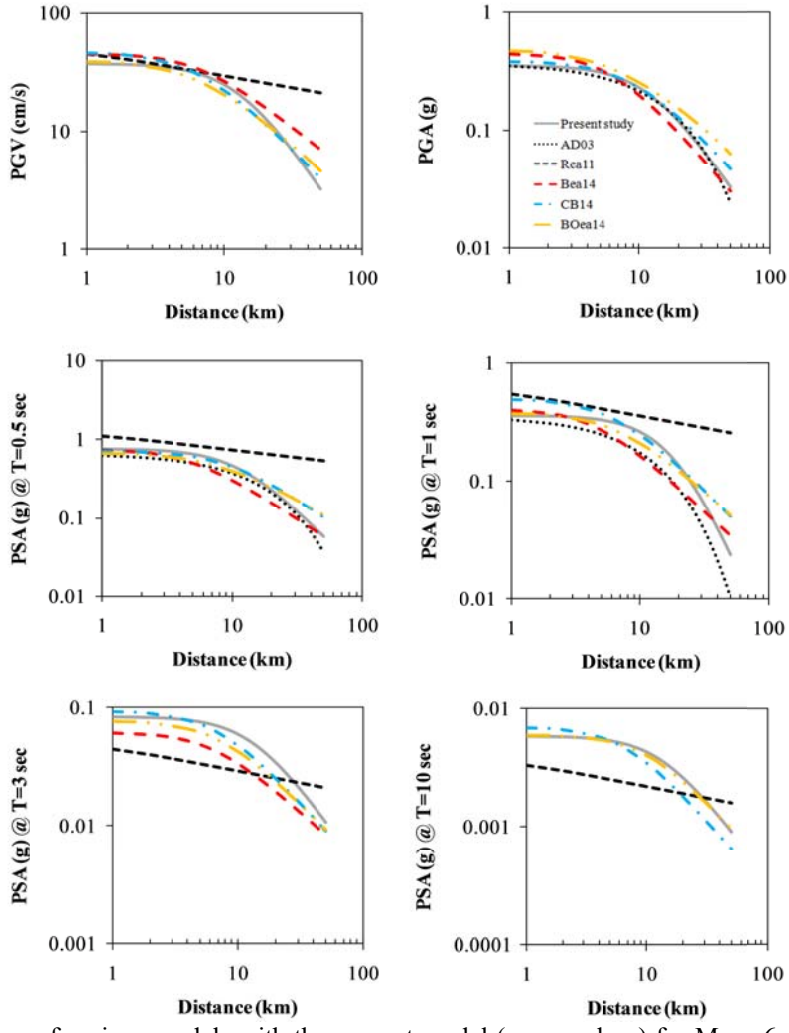

Fig. 10 Comparison of various models with the present model (mean values) for Mw= 6, site class=III and faulting mechanism= strike-slip (S)

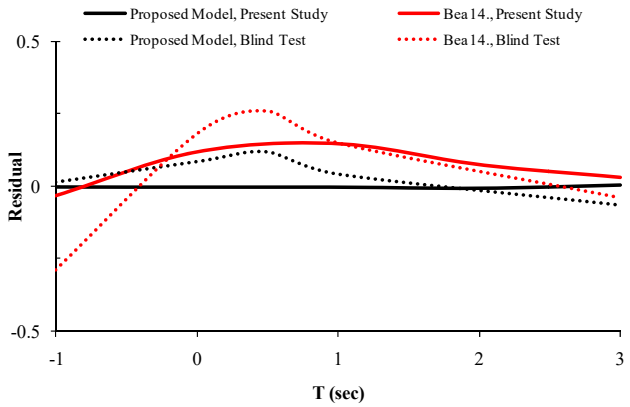

Fig. 11 Comparison of the mean residuals for two models

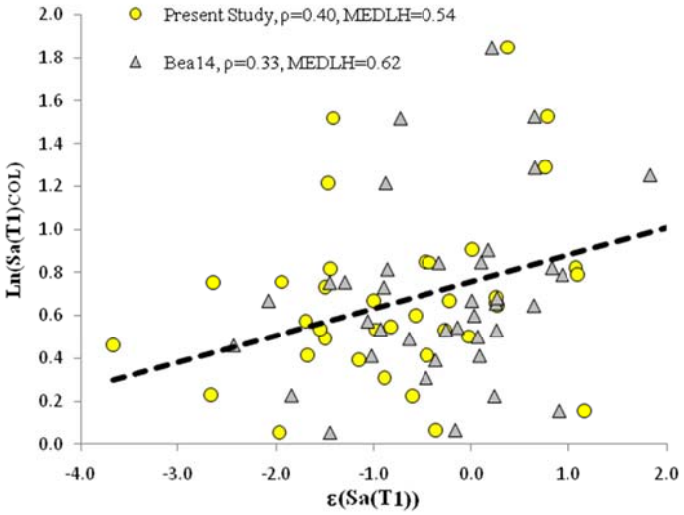

Fig. 12 Comparison of the mean residuals for two models

directly in the calculation of the median collapse intensity at a target ε level (Haselton *et al.* 2009) or implicitly in the structure specific selection of SGMRs for collapse assessment of structures (Mousavi *et al.* 2011). Here, the sensitivity of such correlation to the selection of GMPE for calculation of ε is evaluated. A generic 12-story steel moment frame has been selected from Dimopoulos *et al.* (2012) and is subjected to the vertical irregularity pattern proposed by Chintanapakdee and Chopra (2004) in its lower half by applying strength and stiffness reduction factors of 0.5. The first modal period of model is 1.23s at which the ε values are computed by using our GMPE and Bea14 for a set of 39 SGMRs which have been used in section 5. After incremental dynamic analysis (Vamvatsikos and Cornell 2002) under all SGMs, the estimated Collapse Capacities (CCs) are plotted against corresponding ε values in Fig. 12. The correlation coefficient (ρ) (See section 7) between CC and ε is 0.4; when our model is used to compute the ε, which shows a 21% increase when it is compared to the application of Bea14. Although, more

comprehensive investigations need to be conducted to quantify the sensitivity of such correlations to the selection of GMPEs, it can be inferred that the use of GMPE fitted to the same database used for NLTHA (or effectively selected for database according to the applicability tests) results in more reliable interpretations and conclusions about the structural performance. Fig. 13 compares mean ε values computed for blind test set of ground motions by three GMPEs; our model, Bea14, and Abrahamson and Silva (1997) (Abbreviated as AS97). The latter is widely used in the primitive investigations on the role of spectral shape in collapse simulation. As it is clear in the figure, there is a good agreement between our model and AS97 in periods between 0.5 and 2s, while the differences reveals at short (<0.5s) and long periods (>2s), where the reliability of spectral ordinates may be severely influenced by low quality records.

7. Correlation between IMs

Focusing on the importance of the spectral shape in the performance evaluation of structures; many procedures are proposed to account for this concept through involving spectral shape indicators in the selection and modification (e.g., scaling) of input SGMRs for practical uses, such as, the conditional mean spectrum (CMS) (Baker 2010), Eta-based conditional mean spectrum (E-CMS) (Mousavi *et al.* 2012), and generalized conditional intensity measure (GCIM) approach (Bradley 2010). Such calculations require knowledge of correlation coefficients between different ε_{IM} values (e.g., spectral ordinates at multiple periods) in addition to the valid GMPEs.

There are empirical prediction equations for these correlations which are under the influence of regional differences and sources of uncertainty similar to the developed GMPEs (Baker 2010). In this section, following the development of new GMPE for selected high quality database, the results from the study of observed correlation coefficients and comparison with available empirical predictions are described. A fairly strong correlation between ε_{PGV} and $\varepsilon_{Sa\,(T1)}$ has been reported

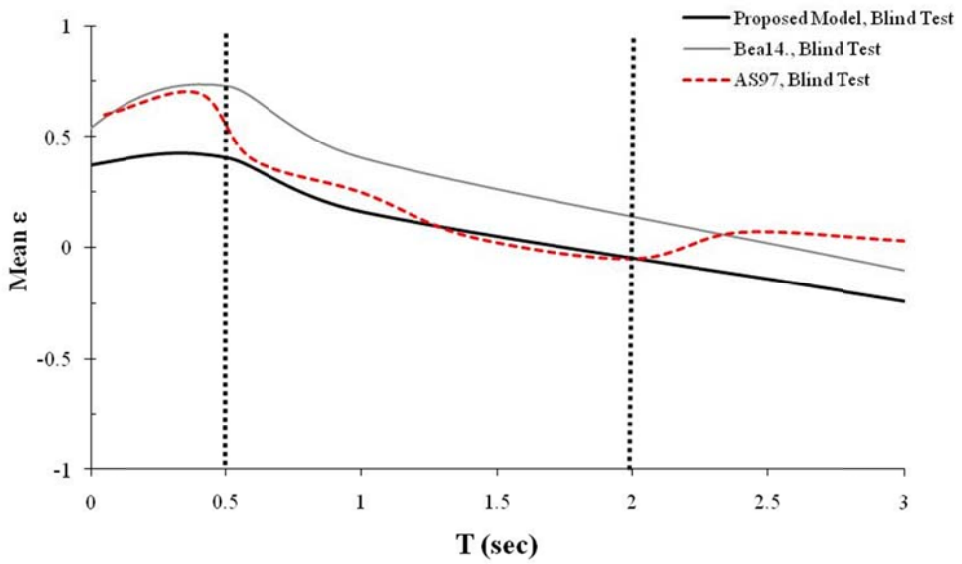

Fig. 13 Gradual variation in mean ε(Sa) computed for Blind test set by using different GMPEs

before (Mousavi *et al.* 2011). Also, it is shown that this correlation can be attained by using an independent-of-period form (ε_{Sa}). Fig. 14 presents observed $\rho_{\varepsilon(PGV),\,\varepsilon(Sa(T1))}$ for 21 periods from 0.01 to 10s that generally confirms presence of correlation, while a very strong correlation ($\rho_{\varepsilon(PGV),\,\varepsilon(Sa(T1))}$=0.93) is obtained by using period independent form of ε_{Sa}. The proposed empirical equation by (Mousavi *et al.* 2011) (with $\rho_{\varepsilon(PGV),\,\varepsilon(Sa)}$=0.73) is plotted in the Fig. 15 indicating its weak predictability for database selected in this paper. To facilitate the generation of conditional spectrum, comprehensive studies have investigated correlation coefficients between spectral ordinates using NGA database and GMPEs (Baker and Jayaram 2008). A predictive equation has been fitted to these data that has been evaluated for some other sets of SGMRs (Jayaram *et al.* 2011). The correlation coefficient between two sets of observed values can be estimated using the maximum likelihood estimator (Kutner *et al.* 2004), also known as, the Pearson product-moment correlation coefficient defined by

$$\rho_{\varepsilon(T_1),\varepsilon(T_2)} = \left[\frac{\sum_{i=1}^{n} (\varepsilon_i(T_1) - \overline{\varepsilon_i(T_1)})(\varepsilon_i(T_2) - \overline{\varepsilon_i(T_2)})}{\sqrt{\sum_{i=1}^{n} (\varepsilon_i(T_1) - \overline{\varepsilon_i(T_1)})^2 \sum_{i=1}^{n} (\varepsilon_i(T_2) - \overline{\varepsilon_i(T_2)})^2}} \right] \tag{8}$$

Using the new proposed GMPE for ground motions of this study, values of $\rho_{\varepsilon(Sa(T1)),\,\varepsilon(Sa(T2))}$ are calculated for different pairs of periods ranging from 0.01 to 10s. Fig. 16 shows the contours of results while the numerical values from this figure are provided in Table A.1 of the appendix. The applicability of empirical prediction equation by Baker and Jayaram (2008) is evaluated by comparing the observed values with their predicted counterparts. Differences computed by Eq. (9) are presented in the contours of Fig. 17

$$Error = \frac{|Observed - Predicted|}{|observed|} \times 100 \tag{9}$$

The perfect performance of the empirical predictions is confirmed for periods up to 1s. The computed error term increases rapidly at longer periods (>3s) that meets about 90% error in the estimated values for T_{max}>5s (T_{max}=Max of T_1 and T_2). This observation is in agreement with the assumption of current study that questions the applicability of predicted spectral ordinates by

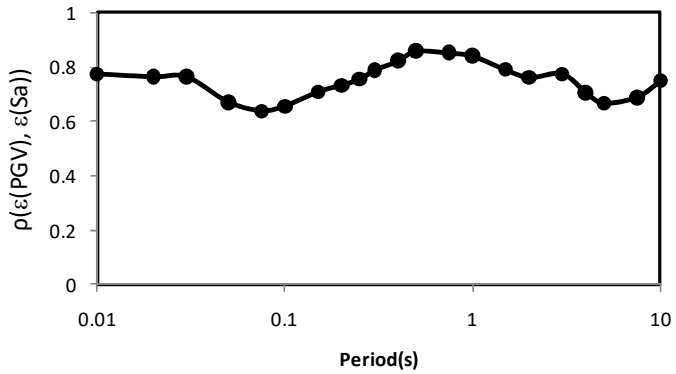

Fig. 14 Variation in $\rho(\varepsilon_{PGV}, \varepsilon_{Sa(T1)})$ calculated by proposed GMPE

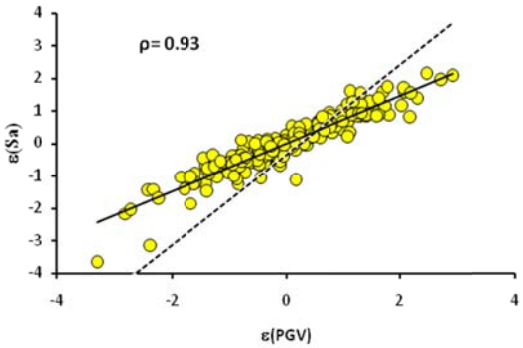

Fig. 15 Correlation between $\varepsilon(Sa)$ and $\varepsilon(PGV)$, dashed line: empirical prediction equation in[15]

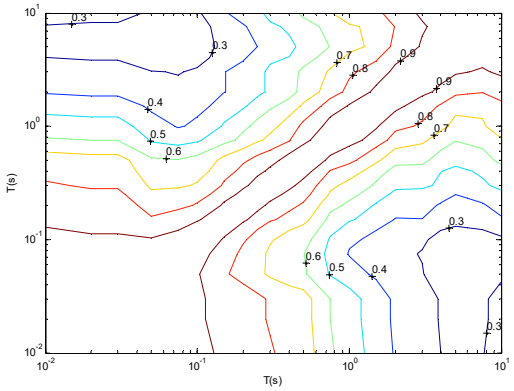

Fig. 16 Contours of correlation coefficients between $\varepsilon(Sa)$ versus T_1 and T_2

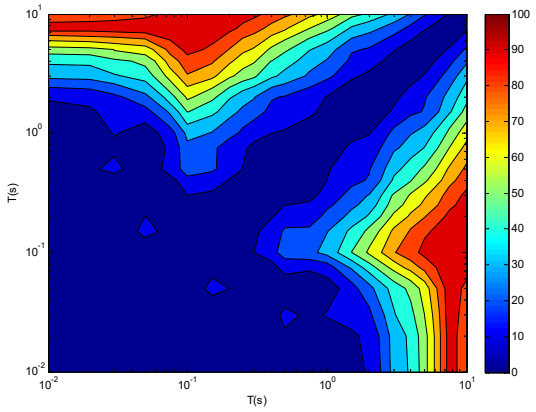

Fig. 17 Contours of computed error from Eq. (9) versus T_1 and T_2

global GMPEs ,especially at longer periods, for refined high quality SGMRs. Separating residuals to the inter-event and intra-event terms enable us to compute correlations for intra-event residuals (ε') as the dominant contributor to the ε (Jayaram *et al.* 2011). The contours of correlation

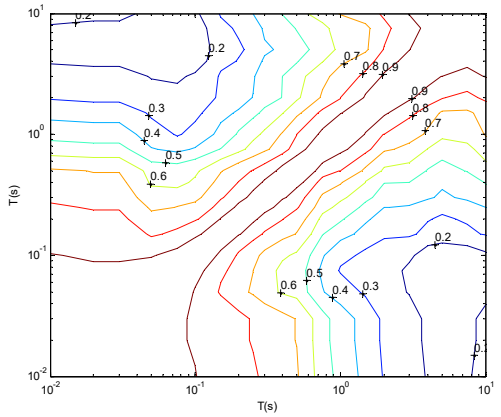

Fig. 18 Contours of correlation coefficients between $\varepsilon'(Sa)$ versus T_1 and T_2

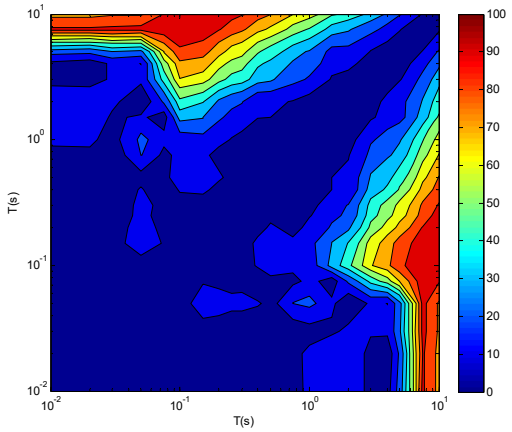

Fig. 19 Contours of computed error from Eq. (9) for ε' versus T_1 and T_2

coefficients for pairs of intra-event normalized residuals and errors to the empirical predictions are plotted in Fig. 18 and Fig. 19, respectively, while the numerical values of coefficients are provided in Table A.2.The overall trend of the results is almost the same as what were computed for ε values, although, slightly weaker correlation is observed at longer periods.

8. Conclusions

A new attenuation model has been developed for *PGV*, *PGA* and 5%-damped *PSA*, using selected high quality data which is refined for dynamic time-history analysis. The advantage of new GMPE is assessed by several goodness-of-fit measures as well as comparison with some global equations selected from literature indicating the general consistency between predictions by new model and others, especially, in short periods. As it should be expected based on the improved reliability of database at longer periods, there are meaningful differences between residuals computed by new model and other empirical equations. A simple example in the case of the

collapse simulation of 12-story steel moment frame shows more than 20% improvement in the observed correlation between collapse capacity and the spectral shape indicators calculated by our model compared to another applicable GMPE fitted to the larger database of SGMRs that is not necessarily refined for time history analysis. The correlation coefficients between pairs of *IMs*, as a requirement for development of conditional intensity models, are computed and compared with available empirical predictions. The applicability of empirical correlation predictions at long periods for used database is deeply questioned by estimated errors that exceed 90% in some cases. New correlation coefficients and more reliable indicators of spectral shape can be utilized by who desire to study the efficiency and sufficiency of modern vector-valued *IMs*, conditional distribution of multiple *IMs* and the concept of structure specific SGMR selection and modification. The fact that a successful prediction equation is fitted to the traditional *IMs* despite the relatively small number of used ground motion records, implicitly, gives insight into the possible future studies to develop reliable GMPEs using this database for more complicated *IMs* dealing with nonlinear response of structures.

Acknowledgments

The research has been funded by the International Institute of Earthquake Engineering and Seismology (IIEES) under Grant Number 604. This support is gratefully acknowledged. Authors are grateful to *Prof. Iunio Iervolino* and *Dr. Chiara Smerzini* for providing ground motions and metafiles of SIMBAD databank. Also, we thank all researchers who have participated to the construction of SIMBAD.

References

Abrahamson, N. and Silva, W.J. (1997), "Empirical response spectral attenuation relations for shallow crustal earthquakes", *Seismol. Res. Lett.*, **68**(1), 94-127.

Abrahamson, N. and Youngs, R. (1992), "A stable algorithm for regression analyses using the random effects model", *Bull. Seismol. Soc. Am.*,**82**(1), 505-510.

Akkar, S. and Bommer, J.J. (2007), "Empirical prediction equations for peak ground velocity derived from strong-motion records from Europe and the Middle East", *Bull. Seismol. Soc. Am.*, **97**(2), 511-530.

Akkar, S. and Bommer, J.J. (2010), "Empirical equations for the prediction of PGA, PGV, and spectral accelerations in Europe, the Mediterranean region, and the Middle East", *Seismol. Res. Lett.*, **81**(2), 195-206.

Ambraseys, N. and Douglas, J. (2003), "Near-field horizontal and vertical earthquake ground motions", *Soil. Dyn. Earthq. Eng.*, **23**(1), 1-18.

Amiri, G.G., Khorasani, M., Hessabi, R.M. and Amrei, S.R. (2009), "Ground-motion prediction equations of spectral ordinates and Arias intensity for Iran", *J.Earthq. Eng.*, **14**(1), 1-29.

Ancheta, T.D., Darragh, R.B., Stewart, J.P., Seyhan, E., Silva, W.J., Chiou, B.S.-J. and Boore, D.M. (2014),"NGA-West2 database", *Earthq. Spectra*, **30**(3), 989-1005.

Baker, J.W. (2010), "Conditional mean spectrum: Tool for ground-motion selection", *J. Struct. Eng.*, **137**(3), 322-331.

Baker, J.W. and Allin Cornell, C. (2006), "Spectral shape, epsilon and record selection", *Earthq. Eng. Struct. Dyn.*, **35**(9), 1077-1095.

Baker, J.W. and Jayaram, N. (2008), "Correlation of spectral acceleration values from NGA ground motion models", *Earthq. Spectra*, **24**(1), 299-317.

Baker, J.W., Lin, T., Shahi, S.K. and Jayaram, N. (2011), "New ground motion selection procedures and selected motions for the PEER transportation research program", Pacific Earthquake Engineering Research Center Report.

Bindi, D., Massa, M., Luzi, L., Ameri, G., Pacor, F., Puglia, R. and Augliera, P. (2014), "Pan-European ground-motion prediction equations for the average horizontal component of PGA, PGV, and 5%-damped PSA at spectral periods up to 3.0 s using the RESORCE dataset", *Bull. Earthq. Eng.*, **12**(1), 391-430.

Bindi, D., Massa, M., Luzi, L., Ameri, G., Pacor, F., Puglia, R. and Augliera, P. (2014), "Erratum to: Pan-European ground-motion prediction equations for the average horizontal component of PGA, PGV, and 5%-damped PSA at spectral periods up to 3.0 s using the RESORCE dataset", *Bull. Earthq. Eng.*, **12**(1), 431-448.

Boore, D.M., Stewart, J.P., Seyhan, E. and Atkinson, G.M. (2014), "NGA-West2 equations for predicting PGA, PGV, and 5% damped PSA for shallow crustal earthquakes", *Earthq. Spectra*, **30**(3), 1057-1085.

Bradley, B.A. (2010), "A generalized conditional intensity measure approach and holistic ground-motion selection", *Earthq. Eng. Struct. Dyn.*, **39**(12), 1321-1342.

Brillinger, D.R. and Preisler, H.K. (1984), "An exploratory analysis of the Joyner-Boore attenuation data", *Bull. Seismol. Soc. Am.*, **74**(4), 1441-1450.

Brillinger, D.R. and Preisler, H.K. (1985), "Further analysis of the Joyner-Boore attenuation data", *Bull. Seismol. Soc. Am.*, **75**(2), 611-614.

Campbell, K.W. and Bozorgnia, Y. (2003), "Updated near-source ground-motion (attenuation) relations for the horizontal and vertical components of peak ground acceleration and acceleration response spectra", *Bull. Seismol. Soc. Am.*, **93**(1), 314-331.

Campbell, K.W. and Bozorgnia, Y. (2008), "NGA ground motion model for the geometric mean horizontal component of PGA, PGV, PGD and 5% damped linear elastic response spectra for periods ranging from 0.01 to 10 s", *Earthq. Spectra*, **24**(1), 139-171.

Campbell, K.W. and Bozorgnia, Y. (2014), "NGA-West2 ground motion model for the average horizontal components of PGA, PGV, and 5% damped linear acceleration response spectra", *Earthq. Spectra*, **30**(3), 1087-1115.

Cauzzi, C. and Faccioli, E. (2008), "Broadband (0.05 to 20 s) prediction of displacement response spectra based on worldwide digital records", *J. Seismol.*, **12**(4), 453-475.

Cauzzi, C., Faccioli, E., Vanini, M. and Bianchini, A. (2014), "Updated predictive equations for broadband (0.01-10 s) horizontal response spectra and peak ground motions, based on a global dataset of digital acceleration records", *Bull. Earthq. Eng.*, **13**(6), 1587-1612.

CEN. (2004), *Eurocode 8: design of structures for earthquake resistance-part 1, General rules, seismic actions and rules for buildings (EN 1998-1)*.

Cheng, Y., Lucchini, A. and Mollaioli, F. (2014), "Proposal of new ground-motion prediction equations for elastic input energy spectra", *Earthq. Struct.*, **7**(4), 485-510.

Chintanapakdee, C. and Chopra, A.K. (2004), "Seismic response of vertically irregular frames: response history and modal pushover analyses", *J. Struct. Eng.*, **130**(8), 1177-1185.

Cantagallo, C., Camata, G. and Spacone, E. (2015), "Influence of ground motion selection methods on seismic directionality effects", *Earthq. Struct.*, **8**(1), 185-204.

Dimopoulos, A.I., Bazeos, N. and Beskos, D.E. (2012), "Seismic yield displacements of plane moment resisting and x-braced steel frames", *Soil. Dyn. Earthq. Eng.*, **41**, 128-140.

FEMA P695 (2009), *Quantification of Building Seismic Performance Factors*, Washington, DC.

Ghafory-Ashtiany, M. and Arian-Moghaddam, S. (2015), "Strong Ground Motion Record Selection; Approaches, Challenges and Prospects", *26th General Assembly of the International Union of Geodesy and Geophysics (IUGG)*, prague, Czech, June 22-July 2.

Ghasemi, H., Zare, M., Fukushima, Y. and Koketsu, K. (2009), "An empirical spectral ground-motion model for Iran", *J. Seismol.*, **13**(4), 499-515.

Graziotti, F., Penna, A. and Magenes, G. (2016), "A nonlinear SDOF model for the simplified evaluation of the displacement demand of low-rise URM buildings", *Bull. Earthq. Eng.*, **14**(6), 1589-1612.

Haselton, C.B. (2006), "Assessing seismic collapse safety of modern reinforced concrete moment frame buildings", Ph.D. Dissertation, Stanford University, Stanford.

Haselton, C.B., Baker, J.W., Liel, A.B. and Deierlein, G.G. (2009), "Accounting for ground-motion spectral shape characteristics in structural collapse assessment through an adjustment for epsilon", *J. Struct. Eng*., **137**(3), 332-344.

Ibarra, L.F. and Krawinkler, H. (2005), "Global collapse of frame structures under seismic excitations", Pacific Earthquake Engineering Research Center Report.

Iervolino, I., Galasso, C. and Cosenza, E. (2010), "REXEL: computer aided record selection for code-based seismic structural analysis", *Bull. Earthq. Eng.*, **8**(2), 339-362.

Jayaram, N., Baker, J.W., Okano, H., Ishida, H., McCann Jr, M.W. and Mihara, Y. (2011), "Correlation of response spectral values in Japanese ground motions", *Earthq. Struct.*, **2**(4), 357-376.

Jayaram, N., Lin, T. and Baker, J.W. (2011), "A computationally efficient ground-motion selection algorithm for matching a target response spectrum mean and variance", *Earthq. Spectra*, **27**(3), 797-815.

Kaklamanos, J. and Baise, L.G. (2011), "Model validations and comparisons of the next generation attenuation of ground motions (NGA-West) project", *Bull. Seismol. Soc. Am.*, **101**(1), 160-175.

Katsanos, E.I., Sextos, A.G. and Manolis, G.D. (2010), "Selection of earthquake ground motion records: A state-of-the-art review from a structural engineering perspective", *Soil. Dyn. Earthq. Eng.*, **30**(4), 157-169.

Kostinakis, K.G. and Athanatopoulou, A.M. (2015), "Evaluation of scalar structure-specific ground motion intensity measures for seismic response prediction of earthquake resistant 3D buildings", *Earthq. Struct*., **9**(5), 1091-1114.

Kutner, M.H., Nachtsheim, C. and Neter, J. (2004), *Applied linear regression models*, McGraw-Hill/Irwin.

Luco, N. and Cornell, C.A. (2007), "Structure-specific scalar intensity measures for near-source and ordinary earthquake ground motions", *Earthq. Spectra*, **23**(2), 357-392.

Kwong, N. Simon and Chopra, A.K. (2016), "Evaluation of the exact conditional spectrum and generalized conditional intensity measure methods for ground motion selection", *Earthq. Eng. Struct. Dyn.*, **45**(5), 757-777.

Mahmoudi, M., Shayanfar, M.A., Barkhordari, M.A. and Jahani, E. (2016), "New fuzzy method in choosing Ground Motion Prediction Equation (GMPE) in probabilistic seismic hazard analysis", *Earthq. Struct*., **10**(2), 389-408.

Medina, R.A. and Krawinkler, H. (2004), *Seismic demands for nondeteriorating frame structures and their dependence on ground motions*, Pacific Earthquake Engineering Research Center.

Mousavi, M., Ghafory-Ashtiany, M. and Azarbakht, A. (2011), "A new indicator of elastic spectral shape for the reliable selection of ground motion records", *Earthq. Eng. Struct. Dyn.*, **40**(12), 1403-1416.

Mousavi, M., Shahri, M. and Azarbakht, A. (2012), "E-CMS: A new design spectrum for nuclear structures in high levels of seismic hazard", *Nucl. Eng. Des.*, **252**, 27-33.

Rupakhety, R., Sigurdsson, S., Papageorgiou, A. and Sigbjörnsson, R. (2011), "Quantification of ground-motion parameters and response spectra in the near-fault region", *Bull. Earthq. Eng.*, **9**(4), 893-930.

Scherbaum, F., Delavaud, E. and Riggelsen, C. (2009), "Model selection in seismic hazard analysis: An information-theoretic perspective", *Bull. Seismol. Soc. Am.*, **99**(6), 3234-3247.

Smerzini, C., Galasso, C., Iervolino, I. and Paolucci, R. (2014), "Ground motion record selection based on broadband spectral compatibility", *Earthq. Spectra*, **30**(4), 1427-1448.

Smerzini, C. and Paolucci, R. (2013), "SIMBAD: a database with selected input motions for displacement-based assessment and design-3rd release", Report of DPC-ReLUIS.

Soghrat, M., Khaji, N. and Zafarani, H. (2012), "Simulation of strong ground motion in northern Iran using the specific barrier model", *Geophys. J. Int.*, **188**(2), 645-679.

Somerville, P.G. (1997), *Development of ground motion time histories for phase 2 of the FEMA/SAC steel project*. SAC Joint Venture.

Vamvatsikos, D. and Cornell, C.A. (2002), "Incremental dynamic analysis", *Earthq. Eng. Struct. Dyn.*, **31**(3), 491-514.

Zafarani, H. and Soghrat, M. (2012), "Simulation of ground motion in the Zagros region of Iran using the specific barrier model and the stochastic method", *Bull. Seismol. Soc. Am.*, **102**(5), 2031-2045.

CC

Appendix

Table A.1 Correlation coefficients between $\varepsilon(Sa)$ versus T_1 and T_2

T_2 ↓ / T_1 →	0.01	0.02	0.03	0.05	0.075	0.1	0.15	0.2	0.25	0.3	0.4	0.5	0.75	1	1.5	2	3	4	5	7.5	10
0.01	1.00	1.00	1.00	0.94	0.92	0.91	0.89	0.86	0.84	0.81	0.78	0.75	0.61	0.55	0.45	0.39	0.37	0.30	0.27	0.29	0.35
0.02	1.00	1.00	1.00	0.94	0.92	0.91	0.88	0.84	0.82	0.79	0.76	0.74	0.60	0.54	0.44	0.38	0.36	0.29	0.26	0.29	0.34
0.03	1.00	1.00	1.00	0.94	0.92	0.91	0.88	0.84	0.82	0.79	0.76	0.74	0.60	0.54	0.44	0.38	0.36	0.29	0.26	0.29	0.34
0.05	0.94	0.94	0.94	1.00	0.95	0.91	0.81	0.76	0.72	0.68	0.64	0.61	0.49	0.44	0.38	0.35	0.30	0.24	0.21	0.24	0.28
0.075	0.92	0.92	0.92	0.95	1.00	0.94	0.84	0.78	0.74	0.68	0.62	0.60	0.46	0.39	0.34	0.32	0.29	0.25	0.23	0.24	0.28
0.1	0.91	0.91	0.91	0.91	0.94	1.00	0.89	0.81	0.76	0.71	0.66	0.63	0.49	0.42	0.37	0.34	0.32	0.26	0.23	0.25	0.29
0.15	0.89	0.88	0.88	0.81	0.84	0.89	1.00	0.92	0.85	0.81	0.77	0.73	0.57	0.51	0.44	0.40	0.40	0.36	0.34	0.36	0.39
0.2	0.86	0.84	0.84	0.76	0.78	0.81	0.92	1.00	0.93	0.88	0.82	0.79	0.63	0.58	0.49	0.43	0.43	0.39	0.37	0.39	0.43
0.25	0.84	0.82	0.82	0.72	0.74	0.76	0.85	0.93	1.00	0.94	0.87	0.83	0.69	0.63	0.54	0.48	0.47	0.43	0.40	0.43	0.48
0.3	0.81	0.79	0.79	0.68	0.68	0.71	0.81	0.88	0.94	1.00	0.92	0.87	0.72	0.67	0.58	0.52	0.52	0.48	0.46	0.48	0.53
0.4	0.78	0.76	0.76	0.64	0.62	0.66	0.77	0.82	0.87	0.92	1.00	0.94	0.79	0.75	0.64	0.56	0.56	0.50	0.48	0.52	0.56
0.5	0.75	0.74	0.74	0.61	0.60	0.63	0.73	0.79	0.83	0.87	0.94	1.00	0.87	0.83	0.72	0.64	0.62	0.56	0.52	0.56	0.62
0.75	0.61	0.60	0.60	0.49	0.46	0.49	0.57	0.63	0.69	0.72	0.79	0.87	1.00	0.93	0.85	0.76	0.72	0.65	0.60	0.63	0.69
1	0.55	0.54	0.54	0.44	0.39	0.42	0.51	0.58	0.63	0.67	0.75	0.83	0.93	1.00	0.91	0.83	0.79	0.73	0.67	0.69	0.75
1.5	0.45	0.44	0.44	0.38	0.34	0.37	0.44	0.49	0.54	0.58	0.64	0.72	0.85	0.91	1.00	0.93	0.85	0.79	0.73	0.72	0.78
2	0.39	0.38	0.38	0.35	0.32	0.34	0.40	0.43	0.48	0.52	0.56	0.64	0.76	0.83	0.93	1.00	0.93	0.88	0.83	0.80	0.84
3	0.37	0.36	0.36	0.30	0.29	0.32	0.40	0.43	0.47	0.52	0.56	0.62	0.72	0.79	0.85	0.93	1.00	0.95	0.91	0.89	0.92
4	0.30	0.29	0.29	0.24	0.25	0.26	0.36	0.39	0.43	0.48	0.50	0.56	0.65	0.73	0.79	0.88	0.95	1.00	0.97	0.93	0.94
5	0.27	0.26	0.26	0.21	0.23	0.23	0.34	0.37	0.40	0.46	0.48	0.52	0.60	0.67	0.73	0.83	0.91	0.97	1.00	0.96	0.95
7.5	0.29	0.29	0.29	0.24	0.24	0.25	0.36	0.39	0.43	0.48	0.52	0.56	0.63	0.69	0.72	0.80	0.89	0.93	0.96	1.00	0.98
10	0.35	0.34	0.34	0.28	0.28	0.29	0.39	0.43	0.48	0.53	0.56	0.62	0.69	0.75	0.78	0.84	0.92	0.94	0.95	0.98	1.00

Table A.2 Correlation coefficients between $\varepsilon'(Sa)$ versus T_1 and T_2

T_1 →

T_2 ↓

Period	0.01	0.02	0.03	0.05	0.075	0.1	0.15	0.2	0.25	0.3	0.4	0.5	0.75	1	1.5	2	3	4	5	7.5	10
0.01	1.00	0.99	0.99	0.93	0.91	0.90	0.88	0.84	0.81	0.78	0.74	0.71	0.54	0.47	0.36	0.29	0.26	0.19	0.16	0.19	0.24
0.02	0.99	1.00	1.00	0.93	0.90	0.90	0.86	0.82	0.79	0.76	0.72	0.70	0.53	0.45	0.35	0.28	0.25	0.17	0.14	0.18	0.23
0.03	0.99	1.00	1.00	0.93	0.90	0.90	0.86	0.82	0.79	0.76	0.72	0.70	0.53	0.45	0.35	0.28	0.25	0.17	0.14	0.18	0.23
0.05	0.93	0.93	0.93	1.00	0.94	0.89	0.79	0.73	0.68	0.64	0.59	0.56	0.41	0.34	0.29	0.25	0.19	0.13	0.10	0.13	0.17
0.075	0.91	0.90	0.90	0.94	1.00	0.93	0.82	0.75	0.70	0.64	0.58	0.55	0.38	0.29	0.25	0.22	0.19	0.14	0.13	0.14	0.17
0.1	0.90	0.90	0.90	0.89	0.93	1.00	0.87	0.79	0.73	0.68	0.61	0.58	0.41	0.33	0.28	0.25	0.22	0.15	0.13	0.15	0.18
0.15	0.88	0.86	0.86	0.79	0.82	0.87	1.00	0.91	0.84	0.79	0.74	0.69	0.51	0.44	0.36	0.32	0.31	0.28	0.26	0.28	0.31
0.2	0.84	0.82	0.82	0.73	0.75	0.79	0.91	1.00	0.93	0.86	0.80	0.76	0.57	0.51	0.42	0.35	0.35	0.31	0.29	0.31	0.35
0.25	0.81	0.79	0.79	0.68	0.70	0.73	0.84	0.93	1.00	0.94	0.86	0.81	0.64	0.57	0.47	0.40	0.39	0.35	0.32	0.35	0.40
0.3	0.78	0.76	0.76	0.64	0.64	0.68	0.79	0.86	0.94	1.00	0.91	0.85	0.68	0.62	0.53	0.45	0.45	0.41	0.39	0.42	0.46
0.4	0.74	0.72	0.72	0.59	0.58	0.61	0.74	0.80	0.86	0.91	1.00	0.93	0.76	0.71	0.60	0.50	0.50	0.44	0.41	0.45	0.50
0.5	0.71	0.70	0.70	0.56	0.55	0.58	0.69	0.76	0.81	0.85	0.93	1.00	0.85	0.80	0.68	0.58	0.57	0.49	0.46	0.51	0.57
0.75	0.54	0.53	0.53	0.41	0.38	0.41	0.51	0.57	0.64	0.68	0.76	0.85	1.00	0.92	0.83	0.72	0.67	0.60	0.55	0.58	0.64
1	0.47	0.45	0.45	0.34	0.29	0.33	0.44	0.51	0.57	0.62	0.71	0.80	0.92	1.00	0.89	0.80	0.75	0.68	0.62	0.64	0.71
1.5	0.36	0.35	0.35	0.29	0.25	0.28	0.36	0.42	0.47	0.53	0.60	0.68	0.83	0.89	1.00	0.91	0.82	0.75	0.69	0.68	0.74
2	0.29	0.28	0.28	0.25	0.22	0.25	0.32	0.35	0.40	0.45	0.50	0.58	0.72	0.80	0.91	1.00	0.91	0.86	0.80	0.77	0.82
3	0.26	0.25	0.25	0.19	0.19	0.22	0.31	0.35	0.39	0.45	0.50	0.57	0.67	0.75	0.82	0.91	1.00	0.94	0.90	0.87	0.90
4	0.19	0.17	0.17	0.13	0.14	0.15	0.28	0.31	0.35	0.41	0.44	0.49	0.60	0.68	0.75	0.86	0.94	1.00	0.97	0.92	0.93
5	0.16	0.14	0.14	0.10	0.13	0.13	0.26	0.29	0.32	0.39	0.41	0.46	0.55	0.62	0.69	0.80	0.90	0.97	1.00	0.95	0.95
7.5	0.19	0.18	0.18	0.13	0.14	0.15	0.28	0.31	0.35	0.42	0.45	0.51	0.58	0.64	0.68	0.77	0.87	0.92	0.95	1.00	0.98
10	0.24	0.23	0.23	0.17	0.17	0.18	0.31	0.35	0.40	0.46	0.50	0.57	0.64	0.71	0.74	0.82	0.90	0.93	0.95	0.98	1.00